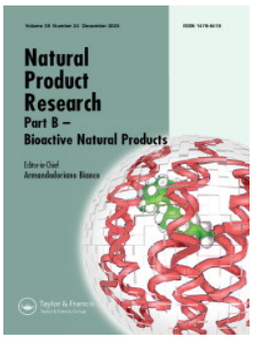

Natural Product Research
Formerly Natural Product Letters

ISSN: 1478-6419 (Print) 1478-6427 (Online) Journal homepage: www.tandfonline.com/journals/gnpl20

# Isolation and characterization of a novel glycoside from the inner bark of *Sclerocarya birrea*: insights into antibiotic and anticancer activity

**Mokgadi Precious Mphahlele, Armand Mallé Lando, Michael Hermann Kamdem Kengne, Jordan Tonga Lembe, Pangaman Jiyane, Thierry Fonkui Youmbi, Vusani Mandiwana, Lerato Hlekelele, Marthe Carine Djuidje Fotsing, Edwin Mpho Mmutlane, Stéphane Zingue & Derek Tantoh Ndinteh**

**To cite this article:** Mokgadi Precious Mphahlele, Armand Mallé Lando, Michael Hermann Kamdem Kengne, Jordan Tonga Lembe, Pangaman Jiyane, Thierry Fonkui Youmbi, Vusani Mandiwana, Lerato Hlekelele, Marthe Carine Djuidje Fotsing, Edwin Mpho Mmutlane, Stéphane Zingue & Derek Tantoh Ndinteh (05 Jul 2025): Isolation and characterization of a novel glycoside from the inner bark of *Sclerocarya birrea*: insights into antibiotic and anticancer activity, Natural Product Research, DOI: 10.1080/14786419.2025.2524608

**To link to this article:** https://doi.org/10.1080/14786419.2025.2524608

NATURAL PRODUCT RESEARCH
https://doi.org/10.1080/14786419.2025.2524608



# Isolation and characterization of a novel glycoside from the inner bark of *Sclerocarya birrea*: insights into antibiotic and anticancer activity

Mokgadi Precious Mphahlele[a,b], Armand Mallé Lando[c], Michael Hermann Kamdem Kengne[a,b], Jordan Tonga Lembe[a,b], Pangaman Jiyane[a,b], Thierry Fonkui Youmbi[d], Vusani Mandiwana[e], Lerato Hlekelele[e], Marthe Carine Djuidje Fotsing[b], Edwin Mpho Mmutlane[f], Stéphane Zingue[g] and Derek Tantoh Ndinteh[a,b]

[a]Centre for Natural Product Research (CNPR), Department of Chemical Sciences, University of Johannesburg, Johannesburg, South Africa; [b]Drug Discovery and Smart Molecules Research Laboratory, Department of Chemical Sciences, University of Johannesburg, Johannesburg, South Africa; [c]Department of Organic Chemistry, Faculty of Science, The University of Yaoundè 1, Yaoundè, Cameroon; [d]Department of Biotechnology and Food Technology, Faculty of Science, University of Johannesburg, Johannesburg, South Africa; [e]Chemicals Cluster, Centre for Nanostructures and Advanced Materials, Council for Scientific and Industrial Research, Pretoria, South Africa; [f]Research Center for Synthesis and Catalysis, Department of Chemical Sciences, University of Johannesburg, Auckland Park, South Africa; [g]Department of Pharmacotoxicology and Pharmacokinetcis, Faculty of Medicine and Biomedical Sciences, University of Yaoundé 1, Yaoundé, Cameroon

**ABSTRACT**

Phytochemical analysis of the dichloromethane-methanol (1:1) extract from *Sclerocarya birrea* inner bark led to the identification of three compounds: a novel glycoside, 3α-sorbithoxyglucose (**1**), and two known compounds, retusasterol (**2**) and *β*-sitosterol-3-*O*-*D*-glycoside (**3**), isolated for the first time from this plant. Structural elucidation *via* NMR confirmed their identities. Cytotoxicity studies against MCF7 breast cancer and DU145, PC3, LNCaP prostate cancer cell lines revealed that compounds **1** and **2** lacked inhibitory effects on cell proliferation, while retusasterol exhibited cytotoxicity with $CC_{50}$ values of 38 µg/mL (DU145), 40 µg/mL (PC3), and 32 µg/mL (LNCaP). However, further analysis indicated that retusasterol promoted tumour cell proliferation. Antimicrobial screening of 3α-sorbithoxyglucose against *Bacillus subtilis*, *Enterococcus faecalis*, *Staphylococcus epidermidis*, *Staphylococcus aureus*, *Mycobacterium smegmatis*, *Enterobacter cloacae*, *Proteus vulgaris*, *Klebsiella oxytoca*, *Klebsiella pneumoniae*, *Proteus mirabilis*, *Escherichia coli*, and *Pseudomonas aeruginosa* revealed MIC values of 15.625–250 µg/mL, suggesting potential as an antimicrobial agent compared to standard antibiotics.

**ARTICLE HISTORY**
Received 3 September 2024
Accepted 19 June 2025

**KEYWORDS**
*Sclerocarya birrea*; novel compound; antibacterial assay; breast cancer; prostate cancer

**CONTACT** Mokgadi Precious Mphahlele mokgadimphahlele25@gmail.com

Supplemental data for this article can be accessed online at https://doi.org/10.1080/14786419.2025.2524608.
This article has been corrected with minor changes. These changes do not impact the academic content of the article.

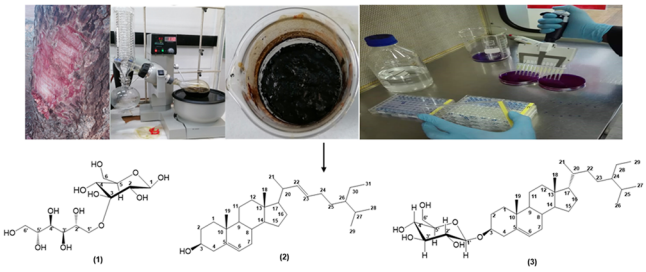

Isolated compounds

| Minimum inhibitory concentration (MIC, ug/mL) | | | | | | | | | | | | |
|---|---|---|---|---|---|---|---|---|---|---|---|---|
| | Gram-positive | | | | | Gram-negative | | | | | | |
| Test sample | *BS* | *EF* | *SE* | *SA* | *MS* | *ECL* | *PV* | *KO* | *PA* | *PM* | *EC* | *KP* |
| Crude extract | 15.63 | 15.63 | 125 | 62.5 | 250 | 125 | 125 | 500 | 500 | 500 | 500 | 500 |
| 3-Mannithoxyglucoside (1) | 15.63 | 15.63 | 250 | 15.63 | 125 | 15.63 | 31.25 | 250 | 15.63 | 125 | 15.63 | 250 |
| Retusasterol (2) | 250 | 250 | 250 | 250 | 250 | 250 | 250 | 250 | 250 | 250 | 250 | 250 |
| AMP | 26 | 26 | 26 | 26 | 26 | 26 | 416 | 26 | 64 | 26 | 26 | 26 |
| STM | 16 | 128 | 8 | 256 | 4 | 512 | 128 | 16 | 128 | 128 | 64 | 512 |
| NLD | 16 | >512 | 64 | 64 | 512 | 16 | 128 | 8 | 128 | 32 | 512 | 256 |

## 1. Introduction

Natural products derived from plants, animals, and microorganisms have played a crucial role in drug discovery, contributing bioactive compounds that serve as the foundation for nearly half of all modern medications, including antibiotics, anticancer agents, and anti-inflammatory drugs. The remarkable chemical diversity and potent biological activities of these natural compounds make them indispensable in addressing global health challenges, such as infectious diseases, cancer, and chronic conditions. Among natural resources, medicinal plants are particularly significant due to their historical role in traditional healing and their continued relevance in pharmaceutical research. One such plant is *Sclerocarya birrea* (A. Rich) Hochst. subspecies *caffra*, commonly known as Marula. This deciduous tree, native to sub-Saharan Africa, is both culturally and scientifically valuable. *S. birrea* belongs to the Anacardiaceae family, which includes other economically and medicinally important plants such as mango (*Mangifera indica*), cashew (*Anacardium occidentale*), and pistachio (*Pistacia vera*) (Mariod et al. 2019). The major constituents of *S. birrea* are phenolic compounds, with phytochemical profiling revealing high concentrations of flavonoids and flavonoid glycosides in methanolic leaf extracts (Russo et al. 2013; 2018). Tannins are predominantly found in the bark and root extracts, while the fruit contains flavonoids, coumarins, tannins, phytosterols, and triterpenoids (Russo et al. 2013; 2018; Daniel et al. 2022). These compounds exhibit a wide range of biological activities, including free radical scavenging, antiallergic, antibacterial, antidiabetic, and anti-inflammatory properties. Notably, procyanidin, isolated from the bark, has demonstrated antidiarrheal activity (Galvez et al. 1993). Detailed phytochemical analysis of the leaves has identified several bioactive compounds, including quercetin 3-*O*-*β*-D-(6″-galloyl)glucopyranoside, quercetin 3-*O*-*β*-D-(6″-galloyl)galactopyranoside, quercetin 3-*O*-*β*-D-glucopyranoside, quercetin 3-*O*-*α*-L-rhamnopyranoside, kaempferol 3-*O*-*β*-D-(6″-galloyl)glucopyranoside, myricetin 3-*O*-*α*-L-rhamnopyranoside, kaempferol 3-*O*-*α*-L-rhamnopyranoside, gallic

acid, (–)-epicatechin 3-O-galloyl ester, and (–)-epigallocatechin 3-*O*-galloyl ester (Braca et al. 2003). GC-MS analysis of the plant's volatile compounds has revealed the highest concentrations of 9-octadecenoic acid, ethyl linoleate, pentasiloxane, carbonic acid, and silane (Njume et al. 2011).

Beyond its phytochemical richness, *S. birrea* is highly valued in African ethnomedicine, where its bark, leaves, and roots have been used to treat ailments such as malaria, fevers, dysentery, diarrhoea, ulcers, headaches, stomach disorders, hypertension, diabetes mellitus, and inflammatory conditions (Eloff 2001; Ojewole et al. 2010; Kpoviessi et al. 2011; Njume et al. 2011; Dabai et al. 2012; Tanih and Ndip 2012; Manzo et al. 2017; Mariod et al. 2019; Adjou et al. 2021; Ghosh et al. 2021; Naidoo et al. 2021). These traditional applications have driven scientific interest in its pharmacological potential, particularly in antibacterial and cytotoxicity studies. Despite its extensive ethnomedicinal use, limited studies have explored the plant's bioactive constituents in-depth. A literature review of published ethnopharmacological data on *S. birrea* is summarised in Table S1. In this study, we report the isolation and characterisation of a novel glycoside compound **1**, retusasterol, and *β*-sitosterol-3-*O*-D-glycoside from the inner bark of *S. birrea*. Additionally, we evaluate the *in vitro* cytotoxicity of compound **1** and retusasterol against breast cancer (MCF-7) and prostate cancer cell lines (DU145, PC3, and LNCaP). Biological assays revealed notable antibacterial activity, further supporting the plant's ethnomedicinal significance. By integrating ethnopharmacological knowledge with natural product chemistry, this study highlights *S. birrea*'s therapeutic potential and underscores its value as a source of bioactive compounds for pharmaceutical development.

## 2. Results and discussion

### 2.1. Structure elucidation of the isolated compounds

The inner bark of *Sclerocarya birrea* was extracted using a 1:1 mixture of dichloromethane and methanol (DCM/MeOH). This extract was then subjected to column chromatography (CC), where a gradient of solvents was used, starting with 100% hexane, followed by increasing proportions of ethyl acetate in hexane, 100% ethyl acetate, then a mixture of ethyl acetate and methanol, and finally 100% methanol. This process led to the isolation of two distinct compounds: retusasterol (**2**) and *β*-sitosterol-3-*O*-D-glycoside (**3**) (Figure S14). Fractions collected from these were mixed and subjected to column chromatography, using 100% chloroform, chloroform: methanol (95:5) to 100% methanol, leading to 3*α*-sorbithoxyglucose (**1**). This compound (222 mg with melting point 187–191 °C) was isolated as a dark red oil using chloroform/methanol (55:45) as a mobile phase. However, the compound gradually precipitated into a shiny, faint pink solid, which was collected from vials MPSB109–114 and subjected to structural analysis. The unusual elution of the disaccharide may have been facilitated by the formation of a ternary mixture, possibly due to trace water in the methanol or silica gel, which enabled the sugar's displacement and subsequent precipitation. The UPLC-QTOFMS obtained using Waters ACQUITY UPLC SYNAPT G2 showed the pseudo molecular ion peak $[M+H]^+$ at *m/z* 361.1353. The FTIR spectrum of compound **1** exhibited O–H groups at 3559 $cm^{-1}$ for free hydroxyl $CH_2$–OH stretch,

O–H stretch at 3320 $cm^{-1}$, and aliphatic CH-groups at 2938 and 2913 $cm^{-1}$. A sharp C-O peak was also observed at 1344 $cm^{-1}$. The $^1$H NMR (500 MHz, $D_2O$) spectrum exhibited signals of oxymethine suggesting that our compound is sugar. Characteristic peaks were observed in the $^1$H spectrum. The peak at $\delta_H$ 5.28 (1H, d, $J$ = 3.9 Hz, H-1), was attributed to the anomeric proton of sugars. Peaks at $\delta_H$ 3.72 (1H, d, $J$ = 3.3 Hz, H-2), $\delta_H$ 4.09 (1H, d, $J$ = 8.9 Hz, H-4), $\delta_H$ 3.76 (1H, ddd, $J$ = 8.4, 6.1, 3.8 Hz, H-5) were attributed to oxymethynes protons H-2, H-4 and H-5 of our first sugar moiety and a broad peak at $\delta_H$ 3.67–3.71 (2H, m, H-6) was assigned to the methylene proton H-6 of our sugar moiety (Noufal 2015; Mailafiya et al. 2020).

A doublet at 5.29 ppm with a small coupling constant ($J$ = 3.9 Hz) suggests that the anomeric proton of the sugar, linked *via* a glycosidic bond, adopts an α-orientation. Moreover, the weak coupling constant $J$ (H-1, H-2) indicates that protons H-1 and H-2 are relatively far from each other, resulting in a weaker spin-spin interaction. This suggests that H-2 adopts an axial position, as its coupling constant ($J$ = 3.3 Hz) is similar to that of H-1 ($J$ = 3.9 Hz), which is in the equatorial position. On the same spectrum, peaks were observed at $\delta_H$ 3.54 (2H, d, $J$ = 8.8 Hz, H-1′), 3.43 (1H, dd, $J$ = 3.8, 10.0 Hz, H-2′), 3.92 (1H, t, $J$ = 8.6 Hz, H-3′), 3.63 (1H, t, $J$ = 8.6 Hz, H-4′), 3.34 (1H, t, $J$ = 9.5 Hz, H-5′) and 3.67-3.71 (2H, m, H-6′) and were assigned to the aglycone moiety (Sarı et al. 2011). The attribution of these peaks is confirmed by the $^{13}$C NMR and DEPT 135 spectra where a total of 12 carbon peaks were observed and attributable to two units: glycone and aglycone. Amongst those peaks, two anomeric carbon peaks were observed at $\delta_C$ 92.2 and 103.7, three methylene carbon peaks at $\delta_C$ 60.1 (C-6′), 61.4 (C-1′) and $\delta_C$ 62.4 (C-6); eight methyne peaks at $\delta_C$ 92.2 (C-1), 73.6 (C-2), 76.5 (C-4), 81.8 (C-5), 71.1 (C-2′), 74.0 (C-3′), 72.4 (C-4′) and 69.2 (C-5′) (Mailafiya et al. 2020). DEPT 135 did not display the peak of the carbon appearing on the $^{13}$C NMR spectrum at $\delta_C$ 103.7 (C-3) suggesting that it is tetra substituted, hence attached to the aglycone unit. The HMBC and HSQC spectra showed some important correlations enabling us to link the two moieties. Amongst those correlations, we observed associations between the anomeric proton $\delta_H$ 5.28 (1H, d, $J$ = 3.9 Hz, H-1) and the carbons $\delta_C$ 103.7 (C-3) and 73.6 (C-2) protons at $\delta_H$ 3.67-3.71 (2H, m, H-6) and carbons $\delta_C$ 81.8 (C-5), proton $\delta_H$ 4.09 (1H, d, $J$ = 8.9 Hz, H-4) and carbon $\delta_C$ 81.8 (C-5), $\delta_C$ 61.4 (C-1′), proton $\delta_H$ 3.76 (1H, ddd, $J$ = 8.4, 6.1, 3.8 Hz, H-5) and carbon $\delta_C$ 103.7 (C-3), proton $\delta_H$ 3.54 (2H, d, $J$ = 8.8 Hz, H-1′) and carbon $\delta_C$ 103.7 (C-3) (Sarı et al. 2011; Mailafiya et al. 2020). An important correlation was also observed between 3.34 (1H, t, $J$ = 9.5 Hz, H-5′) and carbons 72.4 (C-4′) and 60.1 (C-6′). The absolute configuration of compound 1 is determined by its NOESY spectrum (Figure S18). Furthermore, spatial correlations of proton H-1 with H-2, H-4 and H-2′ are observed in this NOESY spectrum (Figure S18). The correlation of proton H-4 with proton H-3′ and that of proton H-3′ with proton H-4′ are also observed in the NOESY spectrum (Figure S18). Based on the $^1$H and $^{13}$C NMR spectral data (Table S2), the structure of compound 1 was assigned to 3$\alpha$-sorbithoxyglucose, a novel glycoside.

Retusasterol **2** ($C_{31}H_{52}O$) (310 mg) was isolated as a pure white powder soluble in chloroform and dissolved in $CDCl_3$. (Ridhay et al. 2012; Noufal 2015).

*β*-Sitosterol-3-*O*-D-glycoside **3** ($C_{35}H_{60}O_6$) (60 mg) dissolved in MeOD, was isolated as a sticky dark red oil which dried out later to dark red crystalline solid (Ridhay et al. 2012; Noufal 2015).

### 2.2. Antibacterial assay

The crude extract of *Sclerocarya birrea* and its isolated compounds were assessed for antibacterial activity against pathogenic bacterial strains. The extract demonstrated notable inhibitory effects, with minimum inhibitory concentrations (MICs) of 15.63 and 62.5 µg/mL against *Bacillus subtilis*, *Enterococcus faecalis*, and *Staphylococcus aureus*. MIC values of 125 µg/mL were observed for *Staphylococcus epidermidis*, *Enterobacter cloacae*, and *Proteus vulgaris*. Compound **1** was evaluated against five Gram-positive and seven Gram-negative bacterial strains in Table S2. This glycoside with a sugar moiety exhibited significant antibacterial activity, with the lowest MIC value of 15.625 µg/mL recorded for *B. subtilis*, *E. faecalis*, *S. aureus*, *E. cloacae*, *Pseudomonas aeruginosa*, and *Escherichia coli*. Higher MIC values were observed for *P. vulgaris* (31.25 µg/mL), *Mycobacterium smegmatis*, and *Proteus mirabilis* (125 µg/mL), while *S. epidermidis*, *Klebsiella oxytoca*, and *K. pneumoniae* required 250 µg/mL for inhibition. Standard antibiotics (nalidixic acid, streptomycin, and ampicillin) were used as positive controls, with MIC values ranging between 4 and >512 µg/mL, depending on the strain. Compound **1** demonstrated greater potency against certain Gram-positive and Gram-negative strains compared to these controls.

The antibacterial efficacy of compound **1** is attributed to its sugar moiety, which contains hydroxyl groups known to enhance aqueous solubility and facilitate passage through bacterial cell walls (Ngah et al. 2022). This characteristic is particularly effective against Gram-negative bacteria, whose hydrophilic periplasmic space typically hinders the entry of lipophilic compounds. Unlike many natural compounds that predominantly target Gram-positive bacteria, compound **1** disrupted the cell walls of both Gram-positive and Gram-negative strains due to its polar structure (Masoko et al. 2010; Ngah et al. 2022). Conversely, retusasterol (compound **2**) exhibited negligible antibacterial activity across all tested strains.

### 2.3. Cytotoxicity in MCF7 cells

The results, derived from triplicate assays, are presented as the arithmetic mean with its associated standard deviation. MCF7 cells were subjected to treatments with compounds **1** and **2** at escalating concentrations of 0.008, 0.016, 0.031, 0.063, and 0.125 mg/mL. A sub-100% cell viability reading was observed for compound **1** at the nadir concentration of 0.008 mg/mL, as illustrated in Figure S15. Cell viability was above 100% after 24 h incubation with retusasterol. The results depicted in Figure S16 show that prolonging the incubation of the retusasterol in MCF7 cells led to enhanced cell proliferation. The sample has shown to be non-toxic at all the treatment concentrations, therefore safe to administer at concentrations between 0.008 and 0.125 mg/mL.

All plant samples assayed in MCF7 cell lines exhibited high rates of proliferation and sustained viability. Ideally, it is expected that the samples would be cytotoxic to both HER-2 positive and negative cell lines. Nonetheless, higher cytotoxicity would be expected in HER-2 positive cell lines, indicating that the compounds can target HER-2 tumours. In this instance, the results suggest that it may be necessary to increase the concentrations of the samples to attain the desired cytotoxicity against

breast cancer cell lines like MCF7 and BT474, while still ensuring safety within non-cancerous cell lines.

### 2.4. Cytotoxicity in DU145, PC3, LNCaP

Retusasterol's cytotoxic potential was assessed against the DU145, PC3, and LNCaP prostate cancer cell lines. Cytotoxicity was observed, with half-maximal cytotoxic concentrations ($CC_{50}$s) of 38 µg/mL for DU145, 40 µg/mL for PC3, and 32 µg/mL for LNCaP cells (Table S5). Across all three cell lines, the compound's inhibitory effect on cell proliferation was both concentration-dependent and statistically significant ($p < 0.01$). This cytotoxic action intensified with increasing incubation time (Figure S17). Peak activity was noted at 10 and 20 µg/mL in DU145 and PC3 cells, respectively. LNCaP cells, however, exhibited maximal growth suppression at 2.5 and 20 µg/mL.

The cytotoxicity of retusasterol was assessed using the MTT assay, which evaluates cell viability by measuring cellular metabolic activity and protein production (Weyermann et al. 2005). The results indicated a concentration- and time-dependent reduction in cell growth for all three prostate cancer cell lines. As shown in Figure S17, cell viability exceeded 50% at lower concentrations, confirming the viability of the cells. Interestingly, retusasterol treatment resulted in increased cellular activity and viability at certain concentrations, exceeding 100% in cell viability measurements. Over a 72 h incubation period, the inhibitory effects intensified, and the $CC_{50}$ values increased with prolonged exposure.

## 3. Experimental

### 3.1. General experimental procedures

One-dimensional (1D) and two-dimensional (2D) nuclear magnetic resonance (NMR) spectra were obtained using a Bruker Biospin 600 MHz spectrometer. For carbon-13 (C-13) and DEPT 135 experiments, a signal frequency of 150.9 MHz was used, while other experiments utilised a 600 MHz signal frequency. Residual solvent signals were used as references, with proton chemical shifts at 7.26 ppm for $CDCl_3$, 3.31 ppm for $CD_3OD$, and 2.50 ppm for DMSO-$d_6$, and carbon chemical shifts at 77.00 ppm for $CDCl_3$, 49.00 ppm for $CD_3OD$, and 39.50 ppm for DMSO-$d_6$. Tetramethylsilane (TMS) served as the internal standard. Data acquisition and processing were conducted using TopSpin™ pulse sequences provided by the Bruker NMR system. Thin-layer chromatography (TLC) was performed on aluminium plates pre-coated with silica gel 60-F254. The crude extracts were separated using column chromatography, employing a glass column packed with silica gel (60–120 mesh).

### 3.2. Plant material

*Sclerocarya birrea* inner bark was harvested in March 2020 at the City of Glory Christian Fellowship Church (24.32738° S,29.14391° E) grounds in Lebowakgomo, Limpopo. The inner bark was collected, with a voucher specimen which was identified by Dr Abdulwakeel Ajao and deposited at the Department of Botany and

Plant Biotechnology, University of Johannesburg Herbarium (JRAU), with voucher number Mphahlele MP 0003 (JRAU). The raw materials were washed, cut, and dried at room temperature to preserve as much as possible the integrity of the molecules. The inner bark was ground into a fine powder, packed in polyethylene bags and stored at room temperature. The extraction took place in the Organometallic and Natural Products laboratory at the Faculty of Science of the University of Johannesburg.

### *3.3. Extraction and isolation*

A total of 791.5 g of *Sclerocarya birrea* inner bark was subjected to maceration with a dichloromethane/methanol (1:1) solution for 7 days. The resulting mixtures were filtered using a Buchner funnel and Whatman No. 1 filter paper. The solvents were subsequently evaporated under reduced pressure at 62 °C using a rotary evaporator, yielding a dry extract of 139.64 g as a dark red solid. The crude extract was then processed by silica gel column chromatography using a glass column. The extract, mixed with silica gel, was loaded onto a glass column, and eluted with a stepwise gradient starting with 100% hexane, followed by hexane-ethyl acetate, 100% ethyl acetate, and a final ethyl acetate-methanol mixture. This procedure yielded twenty-eight fractions. The fractions were analysed using thin-layer chromatography (TLC), and they were grouped into several elutes based on their similarity: MPSB1-8, MPSB9-22, MPSB23-31, MPSB32-35, MPSB36-39, MPSB40-59, MPSB60-73, MPSB74-85, MPSB86-92, MPSB93-101, MPSB102-106, MPSB107-116, MPSB117-124, MPSB125-135, MPSB136-139, MPSB140-146, MPSB147-161, MPSB162-167, MPSB168-172, MPSB173-184, MPSB185-193, MPSB194-208, MPSB209-219, MPSB220-225, MPSB226-234, MPSB235-246, MPSB247-258, and MPSB259-263. Fraction MPSB117-124 collected as a light-yellow solution at a mobile phase of 15% ethyl acetate and 85% hexane, later precipitated as a white precipitate, of which returasterol (compound **2**), was obtained. Fraction MPSB259-263 was obtained as a dark red oily fraction at a mobile phase of 100% ethyl acetate, which precipitated after 24 h, washed with methanol and a red crystals *β*-sitosterol-*3*-*O*-D-glycoside (compound **3**) was obtained. All the fractions were combined and mixed with silica, dried and packed with 100% chloroform and silica gel using wet slurry method. The column was eluted with 100% chloroform, chloroform: methanol (95:5) to 100% methanol. Fractions collected were monitored with TLC using 100% chloroform, chloroform: methanol (95:5, 90:10, 85:15, 80:20, 75:25, 70:30, 65:35, 60:40, 55:45, 50:50) and 100% methanol as solvent systems. A total of 22 fractions were collected and labelled MPSB1-6, MPSB7-15, MPSB16-19, MPSB20-21, MPSB22-23, MPSB24-5, MPSB26-27, MPSB28-31, MPSB32-33, MPSB34-37, MPSB38-46, MPSB46-48, MPSB49-50, MPSB51-60, MPSB61-3, MPSB64-75, MPSB76-82, MPSB83-88, MPSB89-96, MPSB97-105, MPSB106-117, and MPSB118-131. Fraction MPSB106-117 and MPSB109-114 were collected as a dark red oil, while vials MPSB109-114 yielded a shiny faint pink precipitate. This was decanted, washed with chloroform and subjected to structural analysis using NMR, FTIR and UPLCMS. The formation of the precipitate may be attributed to subtle solvent interactions, possibly involving trace water present in the methanol or silica gel.

### 3.4. Biological assay

#### 3.4.1. Antibacterial activity

The antibacterial activity of the compounds was assessed using the method described by Fonkui et al. (2018), which involves determining the minimum inhibitory concentration (MIC). In this procedure, resazurin dye is used to monitor bacterial growth, with the colour changing from blue (indicating no growth) to pink (indicating bacterial growth). The presence or absence of colour change was visually observed to determine the extent of bacterial or eukaryotic cell growth. The MIC was recorded as the lowest concentration at which the colour change occurred, indicating inhibition of growth.

#### 3.4.2. Cell culture

*3.4.2.1. Breast cancer: MCF7.* MCF7 HER2-negative cellular populations were propagated within Dulbecco's Modified Eagle Medium (DMEM), augmented with 10% foetal bovine serum (FBS), 100 IU/mL of penicillin, and 100 mg/mL of streptomycin. The cells was sustained at 37 °C within a $CO_2$-enriched incubator and cultivated in T75 $cm^2$ culture vessels. The nutrient medium was replenished at intervals of 48 to 72 h, while cellular proliferation was observed utilising a Zeiss AxioCam Primo Vert Inverted Phase Contrast Microscope (Carl Zeiss, Germany). Upon attaining 80–90% confluence, cellular detachment was facilitated *via* trypsin-EDTA. To achieve this, the spent medium was aspirated, and 6 mL of 0.05% trypsin supplemented with 0.1% EDTA was introduced. The flask was maintained at 37 °C for a period of 5 to 10 min to encourage dissociation. The detached cells were then gently resuspended utilising a Pasteur pipette. The resulting suspension was transferred into a 15 mL centrifuge tube and subjected to centrifugation at 1500 RCF for 5 min. Following removals of the supernatant, the cell pellet was resuspended in complete DMEM. The suspension was then allocated at a 1:15 ratio into a fresh T75 cultured vessel containing pre-warmed complete DMEM, adjusting the final volume to 15 mL. The flasks were subsequently placed in a humidified incubator at 37 °C under a 5% $CO_2$ atmosphere.

*3.4.2.2. Prostate cancer: DU145, PC3 and LNCaP.* DU145 and PC3 cellular models were cultivated in Roswell Park Memorial Institute (RPMI) 1640 medium, enriched with 10% foetal bovine serum (FBS), 100 U/mL of penicillin, 100 µg/mL of streptomycin, and 10 mM HEPES buffer. These cells were preserved at a stable 37 °C within a humidified incubator maintaining a 5% $CO_2$ environment at pH 7.4. Every 3 to 4 days, the RPMI 1640 culture medium in the T75 flasks was refreshed to sustain cellular expansion. For subculturing, once cellular density reached 80–90% confluence, detachment was induced using trypsin-EDTA. The resulting cell suspension was subjected to centrifugation, with the supernatant meticulously removed. The remaining pellet was resuspended in fresh RPMI 1640 medium, and cells were redistributed at a 1:15 ratio into new T75 culture vessels containing pre-warmed complete medium, adjusting the total volume to 15 mL. Priors to experimental procedures, cellular viability was determined using the trypan blue exclusion assay, and cell quantification was performed using a Neubauer counting chamber.

### 3.4.3. Cytotoxicity assay

**3.4.3.1. Breast cancer: MCF7.** MCF7 cells, actively proliferating in the logarithmic phase, were plated in 96-well microplates at a concentration of $1 \times 10^4$ cells/mL and incubated under $CO_2$-enriched conditions for several days. Once the cells reached full confluence, the culture medium was carefully aspirated, and the monolayer was rinsed with fresh medium. Thereafter, 100 µL of fresh complete medium containing graded concentration of plant-derived compounds was introduced. A density of $1 \times 10^4$ cells/100 µL was seeded per well, ensuring adherence over a 48-hour period in antibiotic-free conditions. Upon reaching 80–90% confluence, cells underwent two sequential washes with fresh medium before exposure to the test compounds and their corresponding serial dilutions. Following a 24 h incubation period, cells were washed twice, and 100 µL of complete medium was reintroduced, along with 10 µL of the WST-1 proliferation reagent. The plate was incubated for an additional 2 h at 37 °C within a 5% $CO_2$ atmosphere. The WST-1 assay quantifies cell proliferation by assessing the bioconversion of WST-1 into formazan, a process facilitated by cellular NADH and an electron mediator. The formazan output directly correlates with proliferative activity, where heightened absorbance signifies increased cellular expansion, while diminished signal intensity suggests cytotoxicity from test compounds. Absorbance measurements were recorded at 450 nm using a Tecan Infinite 500 microplate reader (LifeScience, PA, USA), and cell proliferation was analysed per the manufacturer's protocol.

**3.4.3.2. Prostate cancer: DU145, PC3 and LNCaP.** The MTT [3-(4,5-dimethylthiazol-2-yl)-2,5-diphenyltetrazolium bromide] assay was utilised to assess cellular metabolic activity, proliferation, and overall viability. Prostate cancer cells ($1 \times 10^4$ cells/mL in 100 µL) were plated in 96-well tissue culture microplates, with test substances freshly solubilised in 0.01% DMSO and administered at concentrations spanning 0.5 to 20 µg/mL. Untreated wells functioned as negative controls. Following 24, 48, and 72 h of incubation, 0.5 mg/mL of MTT reagent was introduced into wells containing the experimental treatments, followed by a 4 h incubation period. Subsequently, cell lysis were induced using a buffer comprising 10% sodium dodecyl sulphate (SDS) in 0.01 M HCl, after which the plates were incubated overnight at 37 °C within a 5% $CO_2$ atmosphere. Optical absorbance at 570 nm was recorded for each well using an ELISA microplate reader. Each experimental condition was conducted in triplicate and repeated three times to ensure reliability. Final results were expressed as the mean cell count after subtraction of background absorbance values.

### 3.4.4. Statistical analysis

The experiments were performed in triplicate. Data were expressed as mean ± standard deviation. Statistical analysis was carried out using Student's *t*-test and one-way ANOVA to determine the significance of differences. A *p*-value of less than 0.05 was considered statistically significant.

## 4. Conclusion

In this study, one novel and two known compounds were isolated from the inner bark extract of *Sclerocarya birrea*. The isolated compounds exhibited antibacterial activity against both Gram-positive and Gram-negative bacterial strains, with the sugar moiety likely facilitating penetration of Gram-negative cell walls, resulting in a MIC as low as 15.63 µg/mL. *In vitro* cytotoxicity assays on MCF7 breast cancer and DU145, PC3, and LNCaP prostate cancer cell lines revealed that the compounds were non-cytotoxic and, at lower concentrations, promoted cell proliferation. Notably, retusasterol consistently increased cell proliferation across all prostate cancer cell lines without inducing cytotoxicity. These findings provide essential information for determining safe dosage ranges and guiding further studies on the therapeutic potential and safety of these compounds.

## Acknowledgments

We sincerely thank the LC-MS Synapt Facility (Department of Chemistry, University of Pretoria) for their chromatography and mass spectrometry services, generously provided by Dr. Madelien Wooding.

## Disclosure statement

The authors report no potential conflict of interest.

## Funding

This work was financially supported by the National Research Foundation at the University of Johannesburg (Ref: Grant number PSTD240201203454).

## ORCID

Mokgadi Precious Mphahlele http://orcid.org/0000-0001-8988-1905
Michael Hermann Kamdem Kengne http://orcid.org/0000-0002-2883-3173

## References

Adjou ES, Koudoro AY, Nonviho G, Ahoussi ED, Sohounhloue DC. 2021. Phytochemical profile and potential pharmacological properties of leaves extract of Senna italica Mill. Am J Pharmacol Sci. 9(1):36–39.doi:10.12691/ajps-9-1-3

Braca A, Politi M, Sanogo R, Sanou H, Morelli I, Pizza C, De Tommasi N. 2003. Chemical composition and antioxidant activity of phenolic compounds from wild and cultivated *Sclerocarya birrea* (Anacardiaceae) leaves. J Agric Food Chem. 51(23):6689–6695. doi:10.1021/jf030374m.

Dabai Y, Kawo A, Aliyu R. 2012. Phytochemical screening and antibacterial activity of the leaf and root extracts of Senna italica. Afr J Pharm Pharmacol. 6(12):914–918. doi: 10.5897/AJPP11.852.

Daniel JA, Mathiyazhagan J, Anbazhagan M, Jayaraj R, Gothandam K. 2022. Phytochemistry and pharmacology of *Sclerocarya birrea* (A. Rich.) Hochst.: a review. Bioactives Pharmacol Med Plants. 1:139–147.

Eloff J. 2001. Antibacterial activity of Marula (*Sclerocarya birrea* (A. rich.) Hochst. subsp. caffra (Sond.) Kokwaro)(Anacardiaceae) bark and leaves. J Ethnopharmacol. 76(3):305–308. doi:10.1016/s0378-8741(01)00260-4.

Fonkui TY, Ikhile MI, Ndinteh DT, Njobeh PB. 2018. Microbial activity of some heterocyclic Schiff bases and metal complexes: A review. Trop J Pharm Res. 17(12):2507. doi:10.4314/tjpr.v17i12.29.

Galvez J, Crespo M, Zarzuelo A, De Witte P, Spiessens C. 1993. Pharmacological activity of a procyanidin isolated from *Sclerocarya birrea* bark: antidiarrhoeal activity and effects on isolated guinea-pig ileum. Phytother Res. 7(1):25–28. doi:10.1002/ptr.2650070108.

Ghosh P, Poddar S, Chatterjee S. 2021. Morphological features, phytochemical and ethnopharmacological attributes of Tabernaemontana divaricata Linn.: A comprehensive review. J Pharmacogn Phytochem. 10(6):31–36. doi:10.22271/phyto.2021.v10.i6a.14253.

Kpoviessi DSS, Gbaguidi FA, Kossouoh C, Agbani P, Yayi-Ladekan E, Sinsin B, Moudachirou M, Accrombessi GC, Quetin-Leclercq J. 2011. Chemical composition and seasonal variation of essential oil of *Sclerocarya birrea* (A. Rich.) Hochst subsp birrea leaves from Benin. J Med Plants Res. 5(18):4640–4646.

Mailafiya M, Pateh UU, Hassan H, Sule M, Yusuf A, Bila A. 2020. Isolation and Characterization of Stigmasterol glycoside from the root bark of Leptadenia hastata. FUW Trends in Sci Technol J. 5(2):394–398.

Manzo LM, Bako HD, Idrissa M. 2017. Phytochemical Screening and Antibacterial Activityof Stem Bark, Leaf and Root Extract of Sclerocaryabirrea (A. Rich.) Hochst. Int J Enteric Pathog. 5(4):127–131. doi:10.15171/ijep.2017.29.

Mariod AA, Tahir HE, Komla MG. 2019. *Sclerocarya birrea* chemical composition, bioactivities and uses. In Wild fruits: composition, nutritional value and products. p. 219–228. doi:10.1007/978-3-030-31885-7_18.

Masoko P, Gololo SS, Mokgotho MP, Eloff JN, Howard R, Mampuru L. 2010. Evaluation of the antioxidant, antibacterial, and antiproliferative activities of the acetone extract of the roots of Senna italica (Fabaceae). Afr J Trad Compl Alt Med. 7(2):138–148.doi:10.4314/ajtcam.v7i2.50873.

Naidoo CM, Naidoo Y, Dewir YH, Murthy HN, El-Hendawy S, Al-Suhaibani N. 2021. Major bioactive alkaloids and biological activities of Tabernaemontana species (Apocynaceae). Plants. 10(2):313. doi:10.3390/plants10020313.

Ngah L, Tsopgni WDT, Nyobe JCN, Tcho AT, Langat MK, Ndom JC, Mas-Claret E, Sadgrove NJ, Waffo AFK, Phumthum M. 2022. A new antimicrobial phenylpropanol from the leaves of tabernaemontana inconspicua Stapf. (Apocynaceae) inhibits pathogenic gram-negative bacteria. Antibiotics. 11(1):121. doi:10.3390/antibiotics11010121.

Njume C, Afolayan A, Green E, Ndip R. 2011. Volatile compounds in the stem bark of *Sclerocarya birrea* (Anacardiaceae) possess antimicrobial activity against drug-resistant strains of Helicobacter pylori. Int J Antimicrob Agents. 38(4):319–324. doi:10.1016/j.ijantimicag.2011.05.002.

Noufal MA-SZ. 2015. Retusasterol, a novel sterol and glycoside sitosterol isolated from nitraria retusa. Chem Mater Res. 7(11):1–10.

Ojewole JA, Mawoza T, Chiwororo WD, Owira PM. 2010. *Sclerocarya birrea* (A. Rich) Hochst. ['Marula'] (Anacardiaceae): a review of its phytochemistry, pharmacology and toxicology and its ethnomedicinal uses. Phytother Res. 24(5):633–639. doi:10.1002/ptr.3080.

Ridhay A, Noor A, Soekamto NH, Harlim T, Van Altena I. 2012. A stigmasterol glycoside from the root wood of Melochia umbellata (Houtt) Stapf var. degrabrata K. Indones J Chem. 12(1):100–103. doi:10.22146/ijc.21379.

Russo D, Kenny O, Smyth TJ, Milella L, Hossain MB, Diop MS, Rai DK, Brunton NP. 2013. Profiling of phytochemicals in tissues from *Sclerocarya birrea* by HPLC-MS and their link with antioxidant activity. Int Sch Res Notices. 2013(1):283462. doi:10.1155/2013/283462.

Russo D, Miglionico R, Carmosino M, Bisaccia F, Andrade PB, Valentão P, Milella L, Armentano MF. 2018. A comparative study on phytochemical profiles and biological activities of *Sclerocarya birrea* (A. Rich.) Hochst leaf and bark extracts. Int J Mol Sci. 19(1):186. doi:10.3390/ijms19010186.

Sarı A, Biçer A, Lafçı Ö, Ceylan M. 2011. Galactitol hexa stearate and galactitol hexa palmitate as novel solid–liquid phase change materials for thermal energy storage. Sol Energy. 85(9):2061–2071. doi:10.1016/j.solener.2011.05.014.

Tanih NF, Ndip RN. 2012. Evaluation of the acetone and aqueous extracts of mature stem bark of *Sclerocarya birrea* for antioxidant and antimicrobial properties. Evid Based Complement Alternat Med. 2012:1–7. doi:10.1155/2012/834156.

Weyermann J, Lochmann D, Zimmer A. 2005. A practical note on the use of cytotoxicity assays. Int J Pharm. 288(2):369–376. doi:10.1016/j.ijpharm.2004.09.018. 15620877